Acta Chemica Scandinavica A 29 (1975) 21—28

Kinetics of the Ni/Ni(II) Electrode in Acid Chloride Solution

TOR HURLEN and HARALD A. DÅSNES*

Department of Chemistry, University of Oslo, Blindern, Oslo 3, Norway

From stationary potential/rate curves and galvanostatic transients for either reaction direction of the solid Ni/Ni(II) electrode in aqueous solutions of various pH (0 – 3), chloride ion molarity (1 – 3) and nickel(II) molarity (0 – 1) at 25 °C, and from comparisons to previous results, it appears that the charge transfer of this electrode occurs in two consecutive steps with Ni(I) as intermediate, that neither hydroxyl nor chloride ions participate noticeably in the transfer reactions, and that the ion-transfer step Ni/Ni(I) mostly occurs directly at kink sites, whereas the electron-transfer step Ni(II)/Ni(I) is independent of such sites. On this basis, the data suggest some simple functions for the dependence of the kink concentration on the overvoltage and on the reversible potential.

In spite of the Ni/Ni(II) electrode being a frequently studied solid metal/metal-ion electrode, its reaction mechanism under active conditions is not well clarified and understood (recent reviews in Refs.[1,2]). It is thus not yet clear whether its charge transfer occurs in two consecutive steps with Ni(I) as intermediate [2,3] or in one step with divalent nickel ion as charge carrier.[4,5] Nor is it clear whether its reactions are pH-dependent [2–4] or not.[5,7] Unexplained is also the possible participation by chloride and other anions [1,2] and the role played by crystal growth and demolition.[4] The liquid Ni(Hg)/Ni(II) electrode has recently been found to exhibit both a two-step and a one-step charge-transfer mechanism (the former dominating at low and the latter at high numerical overvoltage) and to be essentially free from direct participation by hydroxyl and chloride ions.[8]

In the present work, the above questions are pursued through determinations of stationary potential/rate curves and galvanostatic transients for solid nickel anodes and cathodes in acidified chloride solutions at 25°C (most previous work is at higher temperatures). The rate measurements (by weight change) allow for simultaneous hydrogen evolution [9] and, hence, give improved polarization data and extend the pH-region for access to such data. The transients yield further information, particularly on the interplay by crystal growth and demolition.

EXPERIMENTAL

All experiments were performed at 25 °C in a 100 ml cell and with equipment essentially as previously described.[8] High-purity (99.998 %) nickel rods (Koch-Light and Johnson, Matthey) were used as test electrodes with exposed surface area near 5 cm^2. Immediately before use and re-use the rods were degreased with chloroform, etched for 1 – 3 min in boiling nitric acid solution (15 %), immersed for about 30 min in hot 2 M HCl, washed with double-distilled water, dried with ethanol, and weighed. All chemicals mentioned as well as acid (HCl) and salts (KCl and $NiCl_2$) for test solutions were of p.a. quality. All solutions were made with double-distilled water, de-aerated with purified nitrogen, and stored and used under nitrogen atmosphere.

The experiments include determinations of the corrosion rate of nickel at open circuit in the solutions applied. In experiments with applied current, corrections were made on this basis for corrosion occurring during currentless periods. For stabilization purposes, the test electrode was generally immersed for about half an hour in the test solution prior to application of current.

In anodic runs, the average dissolution rate over the whole period of applied current was generally determined from the weight loss. In

* This paper comprises part of Harald A. Dåsnes' thesis for the academic degree at the University of Oslo 1972.

some cathodic cases (especially at low pH and low current density), the steady deposition rate reached after some time of electrolysis had to be determined from the weight change as a function of time by a series of comparable runs of various duration at the same current density. All weighings were performed on a Sartorius 2404 Semi-Micro Balance. These reaction rates have been transformed to current densities with a charge equivalent of 2F/mol nickel.

Single-step galvanostatic experiments were performed by means of a three-level fast electronic galvanostat (constructed and built at our institute [10]) combined with a Tektronix Type 564B Storage Oscilloscope with type 3A9 differential amplifier and type 3B4 time base for potential/time recording.

RESULTS

Figs. 1 and 2 give examples of potential/time curves obtained at various anodic and cathodic current densities, respectively. Noted on the curves are also the gravimetrically obtained average anodic dissolution rate (Fig. 1) and final steady deposition rate (Fig. 2). For construction of stationary polarization curves, these rates have been combined with the minimum usually exhibited by anodic potential/time curves (Fig. 1) and with the stationary potential finally reached in cathodic runs (Fig. 2), respectively. This implies the assumption that the minimum mentioned is nearest to representing the stationary anodic polarization of completely active nickel.

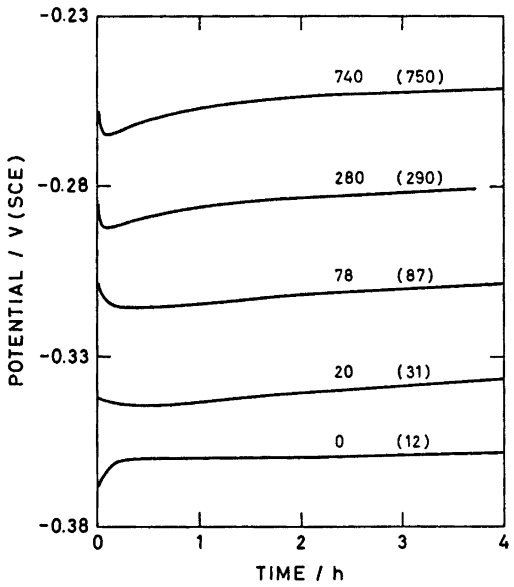

Fig. 1. Anodic potential/time curves in 1 M HCl + 1 M KCl at various applied currents (and average dissolution rates) in μA cm^{-2}.

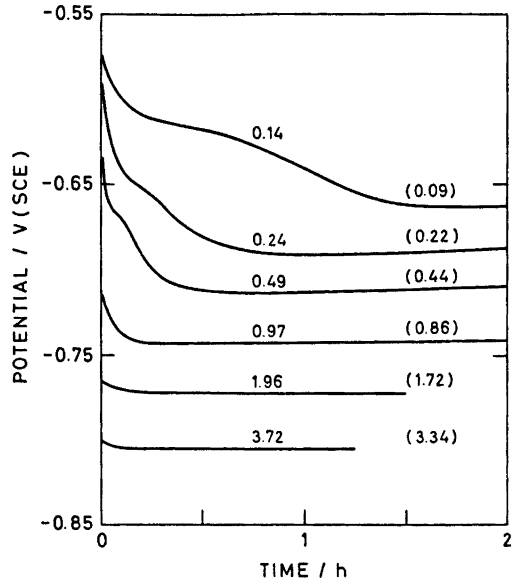

Fig. 2. Cathodic potential/time curves in 0.5 M $NiCl_2$ + 1 M (H+K)Cl of pH about 2 at various applied currents (and final deposition rates) in mA cm^{-2}.

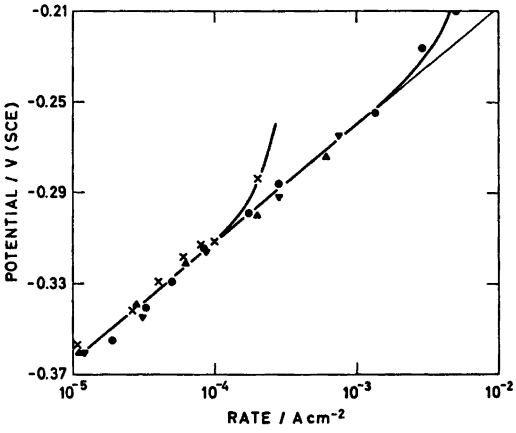

Fig. 3. Potential/rate data for dissolution in (●) 1 M HCl, (▲) 1 M HCl + 1 M KCl, (▼) 1 M HCl + 2 M KCl, and (×) 0.5 M $NiCl_2$ + 1 M (H+K)Cl of pH 2.8.

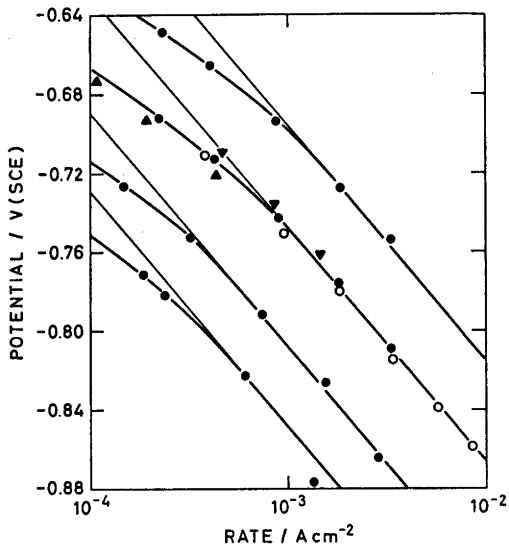

Fig. 4. Potential/rate data for deposition from 2 M chloride solutions of various Ni(II) molarity (1.0, 0.5, 0.2, and 0.1 from top to bottom curve) and pH (▼) 1, (● ○) 2, and (▲) 3; (▼ ●▲) no stirring; (○) stirring.

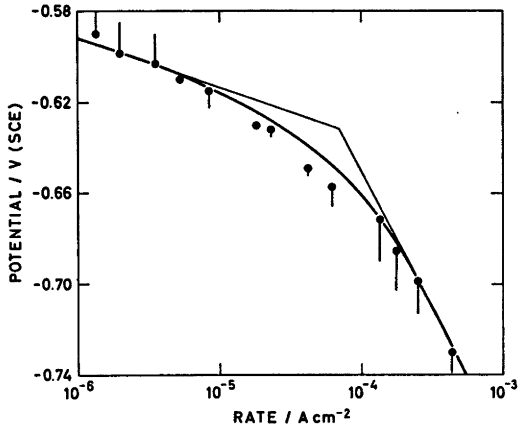

Fig. 5. Potential/rate data for deposition from 0.5 M $NiCl_2$ + 1 M (H+K)Cl of pH 2.8. The curve is calculated (see Interpretations). Corresponding dissolution data in Fig. 3.

Stationary polarization. Fig. 3 gives quasi-stationary polarization data obtained for dissolution of nickel in a number of differently composed chloride solutions. In spite of appreciable differences in pH (0 to 3), in chloride ion molarity (1 to 3) and in nickel(II) molarity (0 to 0.5) for these solutions, the polarization data essentially give one and the same Tafel line for stationary dissolution of active nickel, but show variations in deviations from this line at higher dissolution rates. The line in Fig. 3 has been drawn with a slope of 50 mV per rate decade.

Fig. 4 gives stationary polarization data obtained for deposition of nickel from 2 M chloride solutions of various pH (1 to 3) and nickel(II) molarity (0.1 to 1.0). Also these data appear to be essentially independent of pH. At sufficiently high cathodic overvoltages, the deposition obeys the Tafel law with slope near −120 mV per rate decade and essentially is first order in nickel(II) dependence. At lower cathodic overvoltages, distinct deviations occur from these relationships towards lower Tafel slope and higher nickel(II) dependence.

Fig. 5 gives results of long-time experiments in which the latter deviations are pursued to lower overvoltages and rates in a suitable solution (0.5 M $NiCl_2$ + 1 M (K + H)Cl of pH 2.8). It is suggested that a transition occurs from a Tafel line with slope about −120 mV at high to one with slope −21 mV at low cathodic overvoltages. The latter line intersects with the anodic Tafel line of Fig. 3 at −0.535 V (SCE) and 3×10^{-9} A cm^{-2}. The former line extrapolates to a rate of 7×10^{-6} A cm^{-2}, at the potential mentioned. The two rates may be connected to Ni/Ni(I) and Ni(II)/Ni(I) exhange (see Interpretations).

Galvanostatic transients. Fig. 6 gives examples of the response in potential to a sharp jump in anodic current from a given stationary anodic starting state. A transient superpolarization or potential overshoot clearly follows such a current step and gives a peak in the potential/time curve. In Fig. 7, values obtained for such peak potentials, when starting at one or the other of two different stationary anodic states, are presented in a Tafel diagram. The peak potentials essentially lie on nearly inter-parallel Tafel lines going through the respective starting points and having slopes between 70 and 75 mV per decade.

Analogous studies were performed also on the deposition reaction. A peak (or hump) was then obtained when stepping from a point on

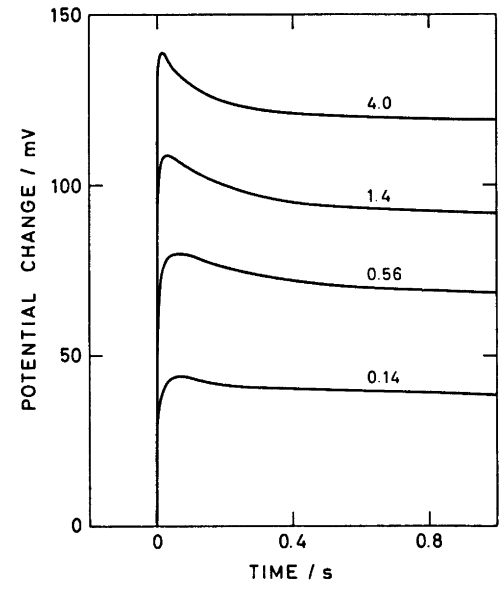

Fig. 6. Potential transients following sharp steps in anodic current to various densities (mA cm^{-2}) from a stationary dissolution rate of 0.04 mA cm^{-2} in 1 M HCl + 1 M KCl.

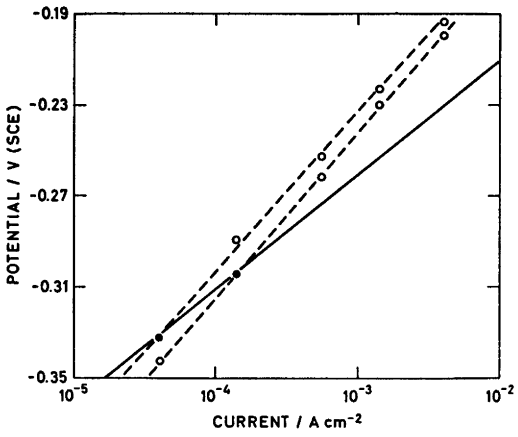

Fig. 7. Anodic peak polarization (○) with one or the other of two different stationary starting states (●) in 1 M HCl + 1 M KCl. The stationary line (fully drawn) is from Fig. 3.

the higher sloped Tafel line to a point on the lower sloped one, but essentially not when stepping reversely to this, nor when stepping between points on the former line. Except for these brief notes, observations on transients are reserved for a more thorough, separate treatment.

INTERPRETATIONS

The stationary polarization data suggest that the charge transfer of the Ni/Ni(II) electrode occurs in two consecutive steps with Ni(I) as intermediate. Together with the transient data, they further suggest that the ion-transfer step Ni/Ni(I) both controls and utilizes kink sites in exposed atom rows, and that the electron transfer step Ni(I)/Ni(II) is independent of such sites. These suggestions shall here be pursued. Attempts of interpretation by several other mechanisms (*e.g.* divalent ion transfer, surface diffusion) have failed.

The above suggestions lead to the following basic rate equations:

$$i_1 = i_{01}(s/s_r)[\exp(\alpha_1 f\eta) - (x/x_r)\exp(-(1-\alpha_1)f\eta)] \quad (1)$$

$$i_2 = i_{02}[(x/x_r)\exp(\alpha_2 f\eta) - \exp(-(1-\alpha_2)f\eta)] \quad (2)$$

for the Ni/Ni(I) step (assuming direct transfer at kinks) and the Ni(I)/Ni(II) step, respectively. In these equations, f means F/RT, x means the appropriate Ni(I) activity, s means the surface concentration of kinks, the subscript r refers to equilibrium conditions, the other symbols have their usual meaning, and signs are chosen so as to make anodic rates positive and cathodic ones negative.

Stationary polarization. If side reactions of Ni(I) can be neglected, steady-state requirements are:

$$i_1 = i_2 = i/2 \quad (3)$$

Provided $i_{01} \ll i_{02}$, eqns. (1) – (3) yield the following stationary Tafel relationships:

$$i = 2i_{01}(s/s_r)\exp(\alpha_1 f\eta) \quad (4)$$

$$i = -2i_{01}(s/s_r)\exp(-(2-\alpha_1)f\eta) \quad (5)$$

$$i = -2i_{02}\exp(-(1-\alpha_2)f\eta) \quad (6)$$

at anodic, moderate cathodic, and high cathodic overvoltages, respectively. Eqn. (5) implies that $x/x_r = \exp(-f\eta)$ at moderate cathodic overvoltages, which means that the Ni(II)/Ni(I) step there exhibits essentially reversible behaviour.

With $\alpha_2 = 0.5$, eqn. (6) shows the Tafel slope observed at high cathodic overvoltages (Figs. 4 and 5). This favours the proposed mechanism. Eqns. (4) and (5) are more involved. Both of them contain the relative surface-concentration of kinks (s/s_r) as a rate factor, and this factor is not yet well known. Good fit is obtained to the observed polarization behaviour, however, if one assumes that the stationary kink concentration obeys an overvoltage relationship of the kind:

$$s/s_r = \tfrac{1}{2}[\exp(\alpha_1' f\eta) + (x/x_r)\exp(-(1-\alpha_1')f\eta)] \quad (7)$$

With this relationship, eqns. (4) and (5) yield $\eta/\ln i$ slopes of $RT/(\alpha_1+\alpha_1')F$ and $-RT/(4-\alpha_1-\alpha_1')F$ at anodic and cathodic overvoltages, respectively. With $\alpha_1 + \alpha_1' = 1.2$, these slopes show the observed values (Figs. 3 and 5). The curve drawn in Fig. 5 has been calculated from the more complete eqns. (1) – (3) with (7) by use of $\alpha_1 = \alpha_1' = 0.6$ and best suiting values for i_{01} and i_{02} (see below).

Reversible exchange and activity effects. From eqns. (4), (5), and (7), it is expected that the stationary anodic Tafel line should intersect with the low-sloped cathodic one at the reversible potential of the Ni/Ni(II) electrode (E) and the exchange current of its Ni/Ni(I) step (i_{01}). The results in 0.5 M $NiCl_2$ + 1 M (H + K)Cl of pH 2.8 (Figs. 3 and 5) accordingly give -0.535 V(SCE) and 3×10^{-9} A cm^{-2} for E and i_{01} in this solution. This E-value is about 40 mV below the standard Ni/Ni(II) potential, which is acceptable enough (considering uncertainties in Ni(II) activity and liquid-junction potential) to satisfy the above expectation. Also this supports the reaction mechanism proposed. Applying eqn. (6) to the high-sloped cathodic Tafel line of Fig. 5, one obtains 3.5×10^{-6} A cm^{-2} for i_{02} in the above solution. This justifies the qualification $i_{01} \ll i_{02}$.

From ordinary electrode kinetics, the proposed reaction mechanism should yield:

$$i_{01} = I_{01}(s_r/s_0)(a/a_0)^{\alpha_1/2} = I_{01}(s_r/s_0)\exp[\alpha_1 f(E-E^\circ)] \quad (8)$$

$$i_{02} = I_{02}(a/a_0)^{(1+\alpha_2)/2} = I_{02}\exp[(1+\alpha_2)f(E-E^\circ)] \quad (9)$$

where a/a_0 is the dimensionless Ni(II) activity (unity at standard conditions) and I_{01}, I_{02}, and s_0 are the values of i_{01}, i_{02}, and s at standard equilibrium of the Ni/Ni(II) electrode. Eqn. (8) will fit observations, provided

$$s_r/s_0 = (x_r/x_0)^{\alpha_1'} = (a/a_0)^{\alpha_1'/2} = \exp[\alpha_1 f(E-E^\circ)] \quad (10)$$

where the latter two equalities follow from thermodynamics.

With eqns. (8) – (10), eqns. (4) – (7) may be transformed to the following stationary Tafel relationships (using $\eta = U - E$):

$$i = I_{01}\exp[(\alpha_1+\alpha_1')f(U-E^\circ)] \quad (11)$$

$$i = -I_{01}(a/a_0)^2\exp[(-(4-\alpha_1-\alpha_1')f(U-E^\circ)] \quad (12)$$

$$i = -I_{02}(a/a_0)\exp[(-(1-\alpha_2)f(U-E^\circ)] \quad (13)$$

at anodic, moderate cathodic, and high cathodic overvoltages, respectively. Eqns. (11) and (13) agree with the experimental results in Figs. 3 and 4, respectively, and their application yields

$$I_{01} = 2 \times 10^{-8} \text{ A cm}^{-2} \quad (14)$$

$$I_{02} = 3 \times 10^{-5} \text{ A cm}^{-2} \quad (15)$$

when -0.495 V (SCE) is used for E°. The activity dependence shown by eqn. (12) has not been tested in the present work, but it agrees with previous results in perchlorate solutions [4] (see below). It moreover must be as written to make eqn. (12) coincide with the confirmed eqn. (11) for $U = E$.

Galvanostatic transients. The occurrence of a peak in a galvanostatic transient is to be expected from the above reaction model when the changes required in s and/or x are slow compared to the double-layer charging. From studies on the Ni(Hg)/Ni(II) electrode,[3] where s is not involved, it appears that changes in x are fast enough and consume little enough current to essentially maintain obedience all the time to the steady-state requirements (3). This makes s the decisive factor, which allows peaks to occur in transients to states obeying eqn. (4) or (5), but not in transients to states obeying eqn. (6). This agrees with the experimental results above.

At a peak ($d\eta/dt = 0$), there is no capacitive current, and the whole current is faradaic. For anodic transients, the current/potential relationship for peaks (the superpolarization) should then be as given by eqn. (4) with s-values between those of the initial and the

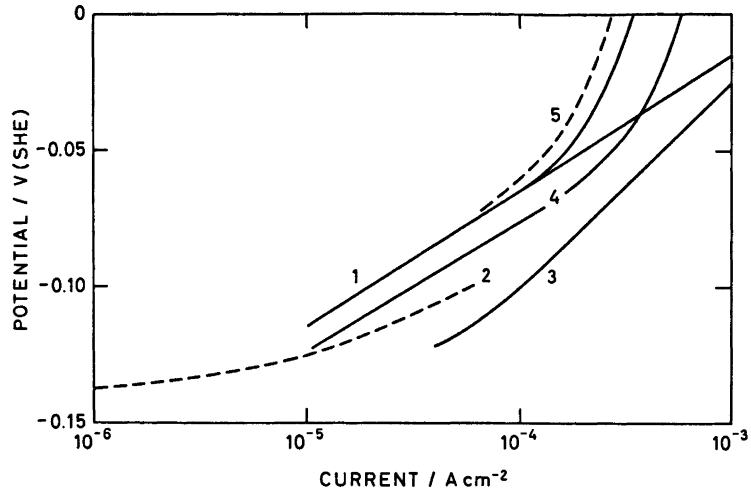

Fig. 8. Anodic polarization data for nickel in various solutions. (1) present work, 1 – 3 M Cl^-, pH 0 – 2.8, 25 °C; (2) Ref. 4, 2 M ClO_4^-, pH 2.5, 65 °C; (3) Ref. 2, 3 M Cl^-, pH 2.1, 60 °C; (4) Ref. 7, 0.5 – 4 M Cl^-, pH 0.6 – 3.0, 55 °C; (5) Ref. 3, 0.5 M SO_4^{2-}, pH 2.75, 40 °C.

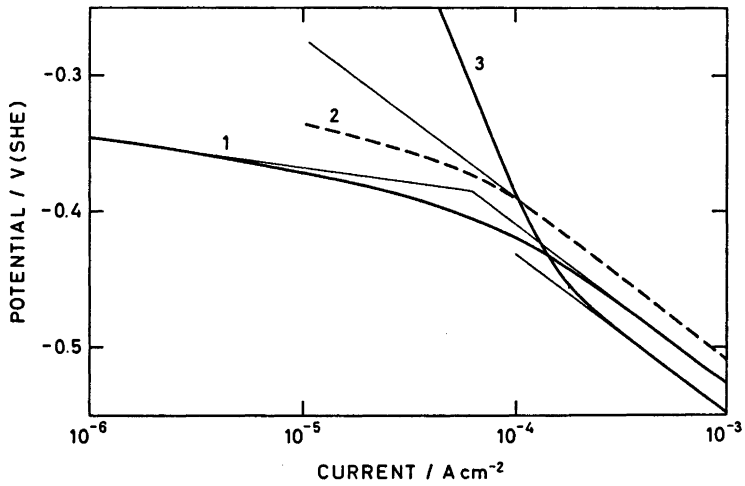

Fig. 9. Cathodic polarization data for nickel in various solutions at 25 °C. (1) present work, 0.5 M $NiCl_2$ + 1 M (H+K)Cl, pH 2.8; (2) Ref. 4, 1 M $Ni(ClO_4)_2$, pH 5.3; (3) Ref. 2, 0.5 M $NiCl_2$ + 2 M NaCl + HCl, pH 2.1.

final steady state concerned. This agrees with Fig. 7.

The present interpretation of the transients implies that the surface concentration of kinks changes appreciably already in the pre-peak period. This concentration is the product of the line density of kinks in crystal steps and the line density of such steps in the surface. The former density should not need much charge to change appreciably and most likely is the one changing in the pre-peak period. This adds to the general appearance of the functions (7) and (10) for s in suggesting that the line density of kinks in crystal steps is an important variable (not merely a temperature-dependent constant).

COMPARISONS

In Figs. 8 and 9, some present and previous quasi-stationary polarization data for nickel electrodes in chloride (solid curves), perchlorate, and sulfate solutions are reproduced for comparison. The standard hydrogen scale has been used, and data from the present work (curves 1) have been transformed to this scale by addition of 0.245 V to values measured on the saturated calomel scale.

Only curves 1 and 4 represent experimentally determined rates of nickel dissolution (Fig. 8) and nickel deposition (Fig. 9). The other curves are ordinary potential/current polarization curves and include some mixing with hydrogen electrode reactions. This particularly applies to curve 2 at low anodic current (Fig. 8) and curve 3 at low cathodic current (Fig. 9). In the former case, a too low Tafel slope and a too high pH-dependence may wrongly be ascribed to the nickel dissolution reaction (see below). In the latter case, hydrogen evolution may well be the main reaction occuring.[5,9]

Anodic data. The anodic data in Fig. 8 apply to various temperatures (25 – 65 °C). A high temperature is often preferred as a means of keeping nickel electrodes active. In the present work at 25 °C, compensations have been sought in the pre-treatment (activation by final etching in hot hydrochloric acid was indispensable), in the experimental procedure, and in the way of choosing representative potentials from potential/time curves. Some previous data [2] for nickel in acid chloride solution at 25 °C are clearly affected by partial passivation even at open circuit (the open-circuit potential reported being positive to the reversible hydrogen potential in the same solution) and are not comparable to the data in Fig. 8. This to some extent applies also to some previous data [3] in acid sulfate solution.

The data in Fig. 8 largely support the conclusions that the stationary dissolution of active nickel has an $U/\ln i$ slope near RT/F and does not involve much participation by hydroxyl and chloride ions. From data like curve 2, however, Heusler and Gaiser [4] derive a lower slope ($RT/2F$) and a second-order hydroxyl-ion interaction, but this may be due to a poor separation of nickel dissolution data from the mixed reaction data actually measured.

Cathodic data. The cathodic data in Fig. 9 all apply to 25 °C. These data combine well in showing that the quasi-stationary deposition of nickel at high current density (or numerical overvoltage) has an $U/\ln i$ slope near $-2RT/F$ and essentially is governed by a pH- and anion-independent first-order reaction of Ni(II). They partly further show that there is a transition to a lower Tafel slope at lower current density in perchlorate as well as in chloride solution. These high-current observations agree with data also at higher temperatures in chloride [5,7] and sulfate [5] solutions, and the low-current ones with data at various temperatures in perchlorate solution.[4] The latter data [4] show that the low-slope region expands with increasing temperature, and that the reaction in this region exhibits a stationary $U/\ln i$ slope between $-RT/3F$ and $-RT/2F$, a transient slope about twice as high, a second-order dependence on Ni(II), but no clear pH-dependence. This agrees with the results and interpretations of the present work [see eqn. (12) above].

DISCUSSION

From the above studies it appears that the charge transfer of the Ni/Ni(II) electrode in the solutions concerned, and within the potential region covered, mostly occurs in two consecutive steps with Ni(I) as intermediate, that neither hydroxyl nor chloride (or perchlorate or sulfate) ions participate specifically in these transfer reactions, and that the ion-transfer step Ni/Ni(I) mostly occurs directly at crystal-growth and -demolition sites, whereas the electron-transfer step Ni(II)/Ni(I) is independent of such sites.

The above mechanism fits both the present and previous results, when due regard is made of simultaneous hydrogen evolution and of partial passivation, and it reconciles much previous controversies on the matter (see Introduction). These controversies, therefore, are not due to conflicting results (as claimed by some authors [11]), but to conflicting interpretations. In subsequent work,[12] the two-step mechanism *via* Ni(I) has been confirmed by stirring, ring-disc, and galvanostatic double-pulse experiments, but the mono-chloro-com-

plex of Ni(II) has been found to enter as electroactive oxidant besides the pure aqua-complex at higher chloride activity and lower water activity than in the present work.

With the above interpretation, the stationary polarization data suggest two relationships, eqns. (7) and (10), which may be combined into the single one:

$$s/s_0 = \tfrac{1}{2}\{[\exp(\alpha_1' f(U-E^\circ)] + (x/x_0)\exp[-(1-\alpha_1')f(U-E^\circ)]\} \quad (16)$$

for the potential and activity dependence of the kink concentration under stationary conditions. This relationship clearly violates the usual assumption of thermal equilibrium of kinks in crystal steps. It rather suggests that kinks are being formed and controlled by electrochemical reactions. To the authors' knowledge, no hitherto treated model directly gives eqn. (16), but some ideas in this direction have been presented.[6,12] More theoretical work is needed on this matter.

With increasing overvoltage, the transfer of divalent nickel ions should be favoured and subsequently gain predominance, as is observed for the liquid Ni(Hg)/Ni(II) electrode.[8] No sign of divalent ion transfer is seen in the present work, however, but the overvoltage region covered is smaller than in the previous amalgam work. The specific rate of electron uptake by Ni(II) appears to be about the same at the solid nickel electrode as at the liquid amalgam electrode. The ion-transfer step Ni/Ni(I) generally is faster than the corresponding Ni(Hg)/Ni(I) step, but not very much so at equilibrium conditions (extrapolated exchange rates). The latter comparison is hampered, however, by Ni(Hg) being in equilibrium with $NiHg_x$ and not with Ni. A striking contrast is the essential absence at solid nickel and clear presence at liquid amalgam of kinetic stimulation by chloride ion adsorption (especially at anodic overvoltages). For both these electrodes, the zero-charge potential lies between most of the actual anodic and cathodic measuring regions.[13]

In closing this discussion, let us briefly consider uni- and divalent ions of the iron-group metals and their immediate neighbours. In weak octahedral ligand fields, the outer electron configurations of these ions and their difference are as given in Table 1.

Table 1. Outer electron configurations.

Metal	M^+	M^{2+}	Diff.
Mn	$t_{2g}^4 e_g^2$	$t_{2g}^3 e_g^2$	t_{2g}
Fe	$t_{2g}^5 e_g^2$	$t_{2g}^4 e_g^2$	t_{2g}
Co	$t_{2g}^6 e_g^2$	$t_{2g}^5 e_g^2$	t_{2g}
Ni	$t_{2g}^6 e_g^3$	$t_{2g}^6 e_g^2$	e_g
Cu	$t_{2g}^6 e_g^4$	$t_{2g}^6 e_g^3$	e_g

The difference shows the type of orbital which accommodates the extra electron of M^+ over M^{2+}. For Mn, Fe, and Co, this is a nonbonding t_{2g} orbital. For Ni and Cu, however, it is an antibonding e_g orbital. The extra electron hence weakens metal-ligand bonds more effectively in the latter cases than in the former ones, and this may correspondingly favour the path via M^+. Such a path does not seem to be used in Fe(Hg)/Fe(II) and Co(Hg)/Co(II) reactions.[14,15]

REFERENCES

1. Erdey-Gruz, T. *Kinetics of Electrode Processes*, Hilger, London 1972, p. 330.
2. Piatti, R. C. V., Arvia, A. J. and Podesta, J. J. *Electrochim. Acta 14* (1969) 541.
3. Sato, N. and Okamoto, G. *J. Electrochem. Soc. 111* (1964) 897.
4. Heusler, K. E. and Gaiser, L. *Electrochim. Acta 13* (1968) 59.
5. Yeager, J., Cels, J. P., Yeager, E. and Hovorka, F. *J. Electrochem. Soc. 106* (1959) 328.
6. Wiart, R. *Oberfläche-Surface 9* (1968) 213, 241 and 275; Epelboin, P. and Wiart, R. *J. Electrochem. Soc. 118* (1971) 1577.
7. Ovari, F. and Rotinyan, A. L. *Elektrokhimiya 6* (1970) 528.
8. Hurlen, T., Eriksrud, E. and Jørgensen, S. *J. Electroanal. Chem. 43* (1973) 339.
9. Dorsch, R. K. *J. Electroanal. Chem. 21* (1969) 495.
10. Grimnes, S. *Chem. Instrum. 5* (1973–74) 141.
11. Davison, W. and Harrison, J. A. *J. Electroanal. Chem. 44* (1973) 431.
12. Hurlen, T. *Electrochim. Acta 7* (1962) 653; *11* (1966) 1205; *20* (1975). *In press.*
13. Perkins, R. S. and Andersen, T. N. In Bockris, J. O'M. and Conway, B. E., Eds., *Modern Aspects of Electrochemistry, No. 5*, Butterworths, London 1969, p. 203.
14. Hurlen, T. and Breiland, B. *J. Electroanal. Chem. 48* (1973) 25.
15. Eriksrud, E. and Hurlen, T. *J. Electroanal. Chem. 36* (1972) 311.

Received July 10, 1974.